ANNALI DI GEOFISICA, VOL. XXXVII, N. 6, December 1994

A model for frictional sliding instability on a heterogeneous fault

Michele Dragoni (1) **and Antonello Piombo** (2)
(1) *Dipartimento di Geologia e Geofisica, Università di Bari, Italy*
(2) *Istituto Nazionale di Geofisica, Bologna, Italy*

Abstract
An instability of frictional sliding driven by tectonic stress is assumed to be the source of earthquakes. Empirical slip laws indicate that, under constant ambient conditions, friction depends on time, slip rate and slip history. Regular stick-slip behaviour is induced by velocity weakening, a decrease of friction with slip rate. Velocity weakening is introduced into a model for a propagating Somigliana dislocation under slowly increasing shear stress in an elastic space. Two distributions of static friction are considered, characterized by asperities with sharp borders and smooth borders respectively. The instability occurs when the rate at which friction decreases becomes greater than the rate at which the applied stress must increase to produce an advance of fault slip. The possibility that this condition is fulfilled depends on the velocity dependence and on the spatial distribution of friction on the fault. In the case of sharp asperity borders, instability can take place only when some amount of slip has occurred on the fault, while this condition is not required in the case of smooth borders.

Key words *dislocation – earthquake – friction – instability – weakening*

1. Introduction

Laboratory experiments and theoretical considerations suggest that earthquakes arise through an instability of frictional sliding on pre-existing rupture surfaces (*e.g.* Scholz, 1990). Experiments show that in frictional sliding of rocks a dynamic instability can occur, resulting in a sudden slip and an associated stress drop. This phenomenon can occur repetitively: the instability is followed by a stationary period during which stress is recharged, followed by another instability. This behaviour is called *stick-slip* and was proposed by Brace and Byerlee (1966) as the mechanism of earthquakes. Earthquakes are recurring slip instabilities on lithospheric faults.

It is commonly assumed that friction τ is locally proportional to the effective normal stress across a fault. The nucleation, the propagation at finite speed and the final arrest of a fault dislocation are necessarily associated with inhomogeneities in friction and/or applied shear stress. Lithological or geometrical changes along the fault are the main causes of spatial changes in friction. Laboratory experiments of the kind initiated by Brace and Byerlee (1966) show that friction of rocks depends mainly on ambient conditions: temperature and pressure in the first place and, in addition, rock type, porosity and pore pressure, thickness of the gouge layer. Frictional sliding may also include the surmonting of obstacles and local processes of fracture or plastic flow (Paterson, 1978).

In general, a dynamic slip instability occurs when the frictional strength decreases at a rate that exceeds the capability of the applied stress to follow (Stuart, 1981). The simplest picture of frictional sliding is that a static friction τ_s must be exceeded for slip to commence. Once slip has started, it is resisted by a dynamic fric-

tion τ_d which is smaller than τ_s. Experiments show however that τ_s and τ_d are not constant in time. If the surfaces are held in stationary contact for a time t, τ_s increases approximately as ln t. During sliding, at constant slip rate v, τ_d is observed to depend on v, being lower for higher slip rates. Moreover the instability does not occur instantaneously at some threshold stress, but after an interval of accelerating slip, and takes place over a finite displacement, the *characteristic slip distance* (Dieterich, 1979a, b; Ruina, 1983; Rice and Ruina, 1983; Rice, 1983; Gu *et al.*, 1984; Weeks and Tullis, 1985).

The frictional behaviour in which friction falls with slip is called *slip weakening* and may result in stick-slip. However it does not provide a mechanism for the frictional resistance to regain its initial level and so does not lead to the regular stick-slip behaviour which is required to explain earthquakes. The basic phenomenon which leads to regular stick-slip is *velocity weakening*, a decrease of friction with increasing slip rate v. If v is an increasing function of time, slip weakening is just a consequence of velocity weakening.

Under constant and uniform ambient conditions, fault strength depends on time, slip rate and slip history (Dieterich, 1978; Ruina, 1983; Weeks and Tullis, 1985). The experimental observations can be represented by constitutive relations including slip rate and slip history effects: the sliding history effects are usually represented by a state variable that evolves with displacement toward a steady-state value. Okubo (1989) worked out a dynamic rupture model with laboratory-derived constitutive relations. Earthquake nucleation on a fault with slip-rate dependent strength was studied with a numerical model by Dieterich (1992) and Matsu'ura *et al.* (1992). Shibazaki and Matsu'ura (1992) developed a numerical simulation for the process of nucleation, dynamical propagation and stop of earthquake rupture.

In the present paper, we introduce an empirical constitutive equation into a model representing a Somigliana dislocation (or crack) propagating on a fault with nonuniform friction, under a slowly increasing ambient shear stress. Two distributions of static friction are studied, characterized by asperities with sharp borders and smooth borders, respectively. The penetration of an aseismic dislocation into asperities with sharp borders was studied in Dragoni (1990, 1992). The case of asperities with smooth borders was considered in Dragoni and Piombo (1993). Here we study the conditions under which sliding instability may take place as a consequence of such an aseismic dislocation process (*e.g.* Dragoni, 1993).

2. The model

We assume that faults are pre-existing rupture surfaces in the Earth's lithosphere and that fault slip is controlled by friction

$$\tau = \kappa(\sigma_n - p) \tag{2.1}$$

where κ is the coefficient of friction, σ_n is the applied normal stress and p is fluid pore pressure. Friction may vary in space as a consequence of changes in κ, σ_n and p. Such a function includes the effect of lithologic and geometric inhomogeneities of the fault as well as of all the other factors controlling the resistance to slip, like fluid pore pressure (Rice and Simons, 1976), fault gouge (Wang, 1984) and possible lithification processes (Angevine *et al.*, 1982).

We consider a planar fault surface in an elastic space and describe the spatial dependence of friction by a combination of weak and strong patches. Fault slip takes place in response to a gradually increasing ambient shear stress. If the ambient stress is uniform, slip starts in the weakest patch of the fault. A Somigliana dislocation (or crack) is produced (Bilby and Eshelby, 1968).

To make the problem amenable to an analytical solution, a 2-D model is considered, where friction is variable only in one direction x on the fault plane, taken as the horizontal direction. We assume that the fault is stationary for $t < 0$. At $t = 0$ the static friction is $\tau_s(x)$: in particular, we assume that there is a weak zone of the fault plane, $-d < x < d$, with friction τ_0, included between stronger zones with friction $\tau_1 > \tau_0$ (fig. 1a,b), that we call «asperities». We

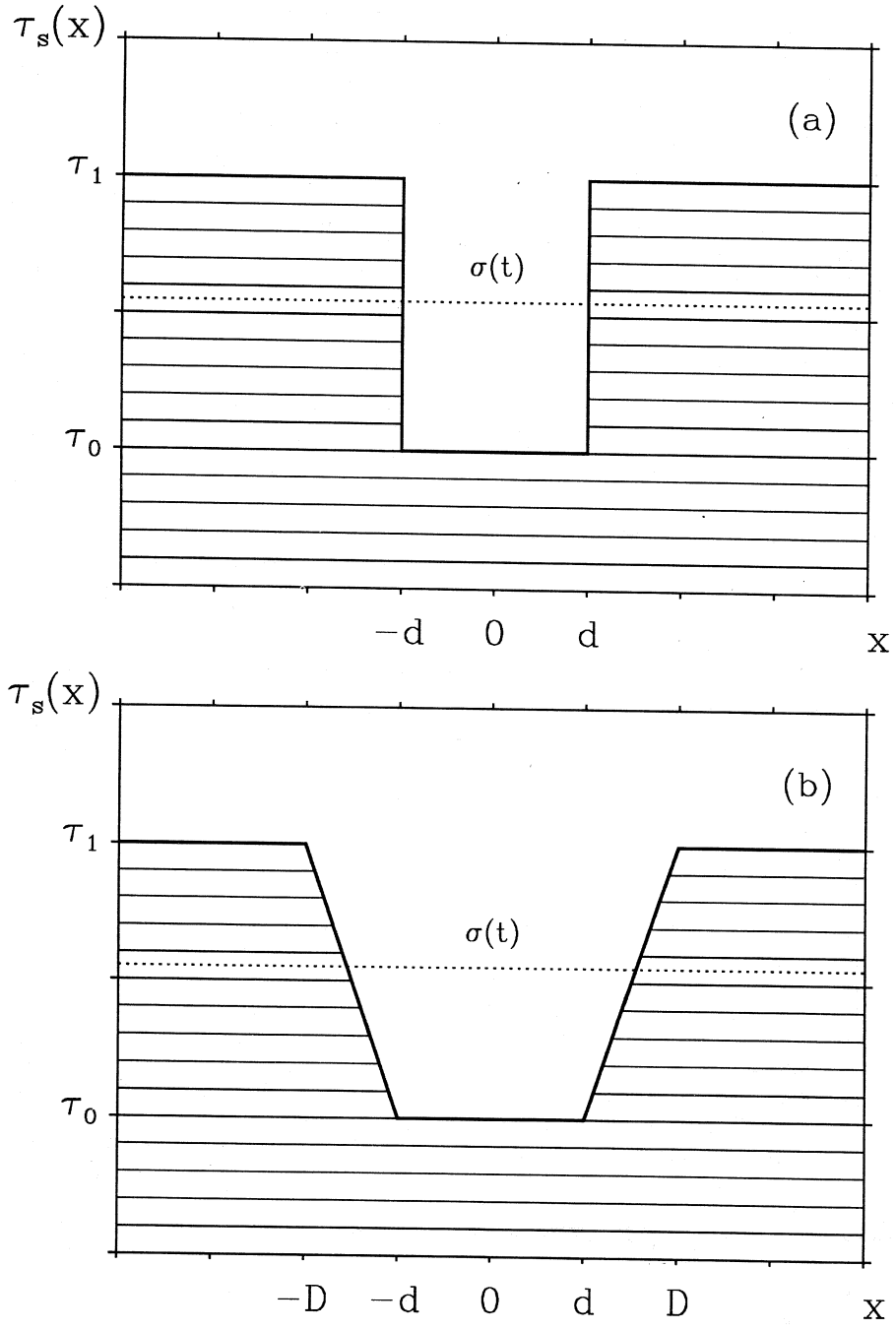

Fig. 1a,b. Static friction $\tau_s(x)$ around the weakest fault zone at time $t = 0$, where x is a coordinate along the fault. We consider two distributions characterized by asperities with sharp borders (a) and smooth borders (b); σ is the ambient shear stress, increasing with time t. It is assumed that $\sigma = \tau_0$ at $t = 0$.

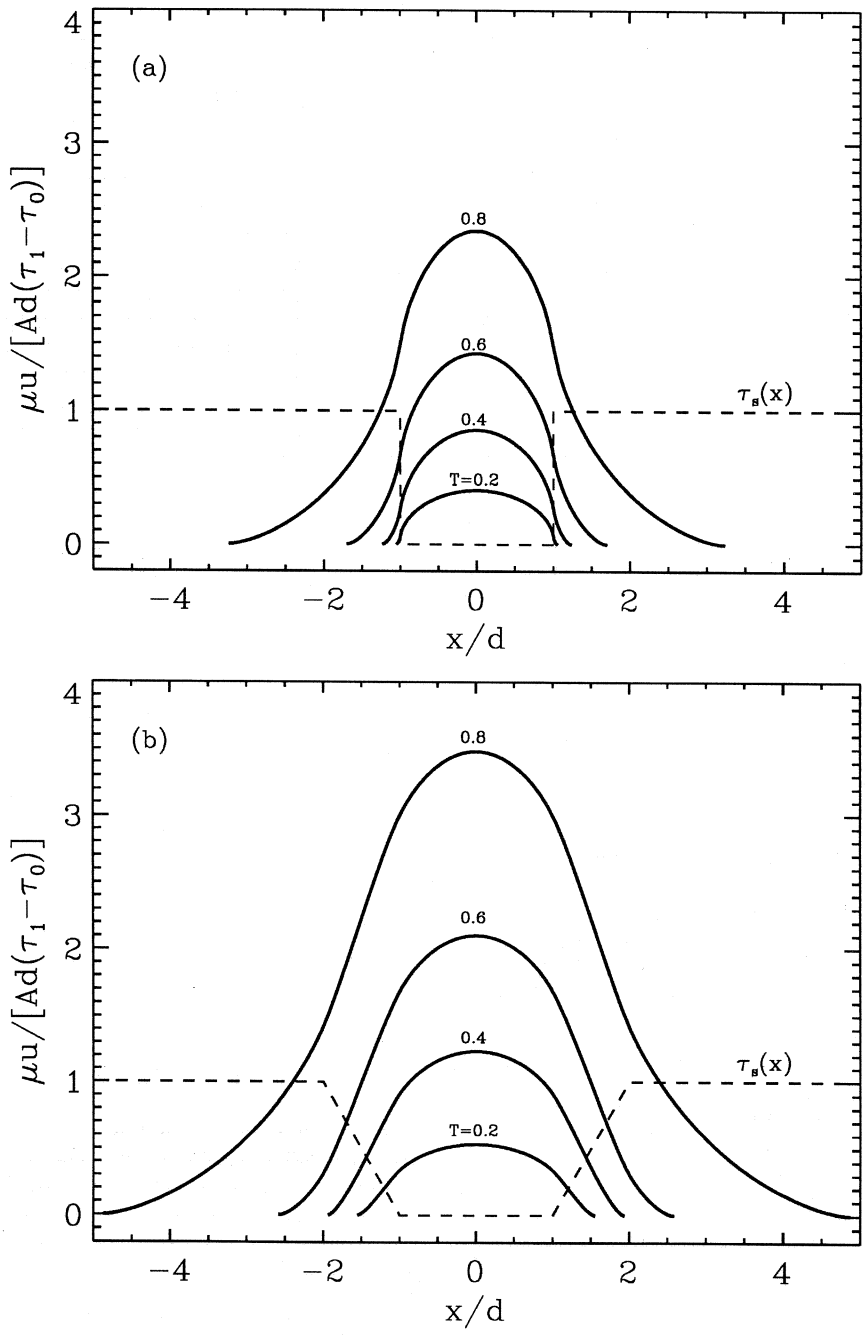

Fig. 2a,b. Fault slip u as a function of coordinate x along the fault, for different values of parameter T (corresponding to different times), in the two cases of sharp asperity borders (a) and smooth asperity borders with $D = 2d$ (b).

consider two cases: asperities having sharp borders with

$$\tau_s(x) = \begin{cases} \tau_0, & |x| < d \\ \tau_1, & |x| > d \end{cases} \qquad (2.2)$$

and asperities having smooth borders, with

$$\tau_s(x) = \begin{cases} \tau_1, & |x| \geq D \\ \tau_0, & |x| \leq d \\ \tau_0 - (x+d)f, & -D \leq x \leq -d \\ \tau_0 + (x-d)f, & d \leq x \leq D \end{cases} \qquad (2.3)$$

where

$$f = \frac{\tau_1 - \tau_0}{D - d} \qquad (2.4)$$

is the friction gradient of the asperity borders, having width $D - d$. We assume moreover that the ambient shear stress σ reaches the value τ_0 at $t = 0$: at that time the fault starts sliding and releasing a stress

$$\Delta\sigma(x, t) = \sigma(t) - \tau(x, t), \quad |x| < a(t) \qquad (2.5)$$

where a is the dislocation half-width and we admit that friction τ may vary as a function of time. Under equilibrium conditions, the increase of dislocation amplitude u and width $2a$ is controlled by the increase of ambient stress σ, the dislocation being confined by the surrounding asperities. The solution technique of the Somigliana dislocation problem is summarized in the Appendix.

In the absence of velocity weakening, the various quantities of the model are usefully expressed in terms of a nondimensional, time-dependent parameter

$$T(t) = \frac{\sigma(t) - \tau_0}{\tau_1 - \tau_0} \qquad (2.6)$$

which is a measure of how much the ambient stress σ exceeds the friction level τ_0, relatively to the step $\tau_1 - \tau_0$. As σ increases from τ_0 to τ_1, the ratio T increases from 0 to 1. If σ is linearly increasing with time, T is equivalent to time and will be used in the following instead of t.

In a Somigliana dislocation, fault slip u and slip rate v are functions of position and of time. Figure 2a,b shows the slip profiles along the fault for different values of parameter T in the two cases of sharp and smooth asperity borders; we note that slip is proportional to $\tau_1 - \tau_0$ and, for a given value of T, u is remarkably larger in the case of smooth asperity borders. In fig. 3a,b the slip rate profiles are shown on the fault for the same values of T; also slip rate is larger for smooth borders at any given value of T. Slip rate is however independent of $\tau_1 - \tau_0$. In figs. 2a,b and 3a,b and in the following, $D = 2d$ is assumed as an example for the smooth border case; u and v are suitably normalized: μ is the rigidity of the elastic medium and A is another elastic constant which is defined in the Appendix. At any time $t > 0$ (or $T > 0$), the maximum fault slip and the maximum slip rate are at $x = 0$, the centre point of the weak zone.

The fault can be characterized by an effective stiffness (Dieterich, 1986), defined as the derivative of ambient stress with respect to fault slip. At fixed t, the minimum stiffness K_σ is found at $x = 0$, where the slip is maximum. Therefore the centre point $x = 0$ may be assumed to control the onset of instability for the entire fault patch and we define

$$K_\sigma \equiv \frac{d\sigma}{dU} \qquad (2.7)$$

where

$$U(t) = u(0, t). \qquad (2.8)$$

A graph of σ as a function of U is shown in fig. 4, whence it can be seen that $K_\sigma > 0$: K_σ represents the increment of ambient shear stress which is needed to produce a corresponding increment of fault slip. This slip hardening effect is produced as a consequence of the propagation through adjacent higher friction zones which resist the motion of dislocation fronts. The dotted line in fig. 4 and in the following refers to the case of smooth border asperities and corresponds to the condition

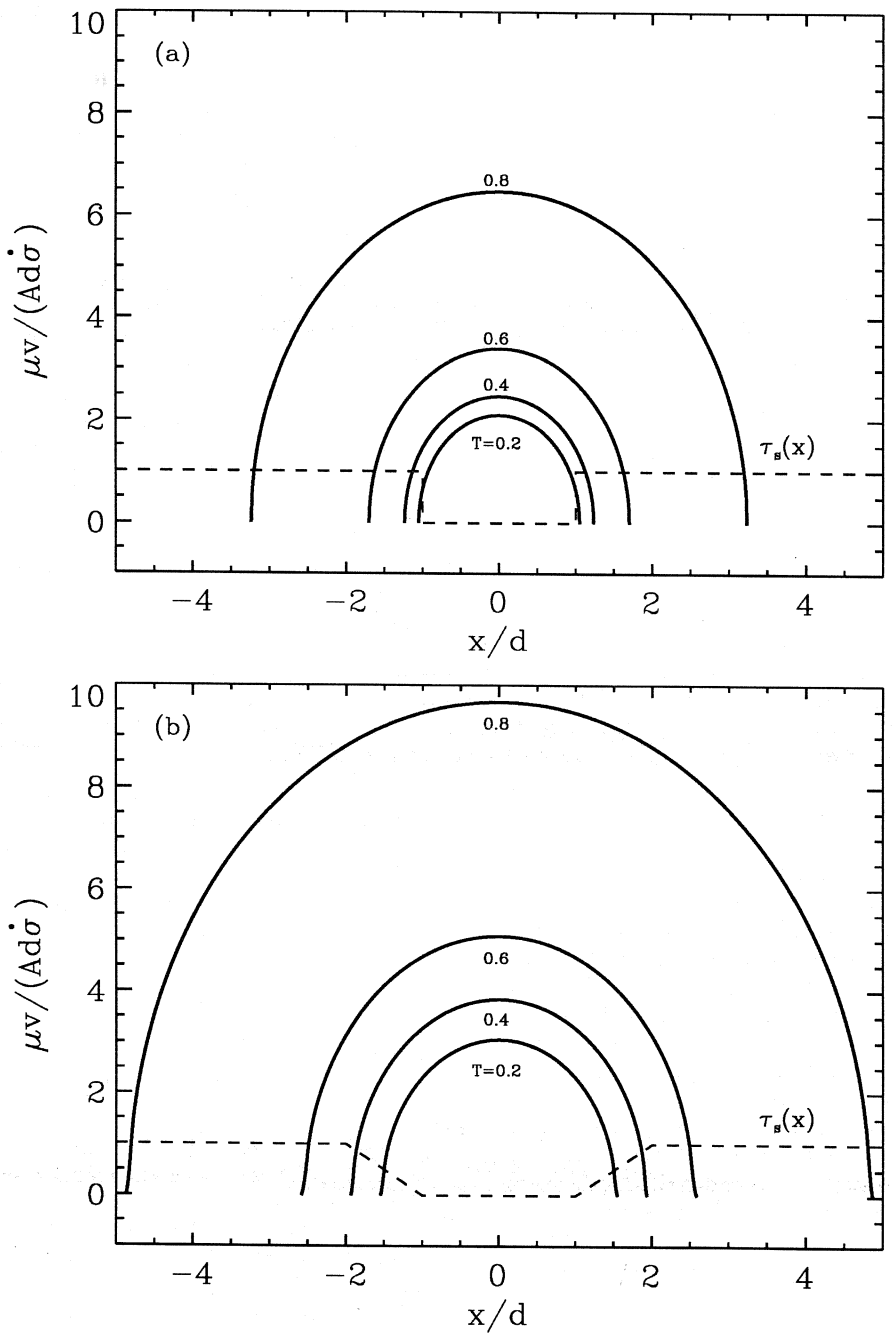

Fig. 3a,b. Fault slip rate v as a function of coordinate x along the fault, for different values of parameter T (corresponding to different times), in the two cases of sharp asperity borders (a) and smooth asperity borders with $D = 2d$ (b).

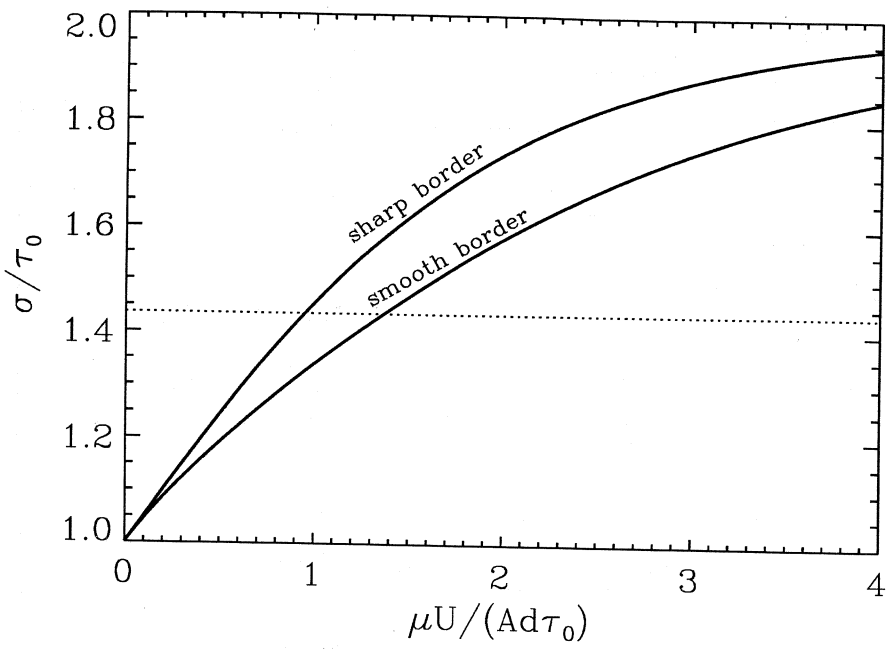

Fig. 4. Stress-slip curves. Two kinds of friction distribution are considered: sharp asperity borders ($(\tau_1 - \tau_0) / \tau_0 = 2$) and smooth asperity borders ($(\tau_1 - \tau_0) / \tau_0 = 2$, $D = 2d$).

$a = D$, when the dislocation front has passed the asperity border.

It can be seen that K_σ depends on τ_0 and τ_1 only through the nondimensional stress release T. Besides, it depends on the elastic constants and on the weak zone half-width d. A graph of the nondimensional quantity AdK_σ/μ as a function of T is shown in fig. 5: K_σ is a bounded function of T and has a maximum

$$\overline{K}_\sigma = \frac{\mu}{2Ad} \tag{2.9}$$

at $T = 0$. The existence of a maximum $\overline{K}_\sigma$ takes into account the possibility that fault slip starts at $t = 0$ on a zone with finite extension $2d$ and not just at a point.

3. Velocity weakening and instability

There are various forms of constitutive equations, which differ in detail, depending on the approximations employed, but all share the same approach and provide similar representations of the data. A typical form of constitutive law, yielding the coefficient of friction κ in terms of slip rate v and a state variable ψ, is the following:

$$\kappa = \kappa_0 + \mathcal{A} \ln g(v) + \mathcal{B}\psi \tag{3.1}$$

where κ_0 is some basic friction, $\mathcal{A}$ and $\mathcal{B}$ are empirically determined constants and $g(v)$ is a function of v. The constitutive equation is accompanied by an equation for the evolution of the state variable ψ:

$$\frac{d\psi}{dt} = -\frac{v}{\ell}[\psi + \ln g(v)] \tag{3.2}$$

where ℓ is the characteristic slip distance which is measured in the laboratory (*e.g.* Scholz, 1990). A more general formulation may involve several state variables, each obeying to its own constitutive equation (Horowitz and

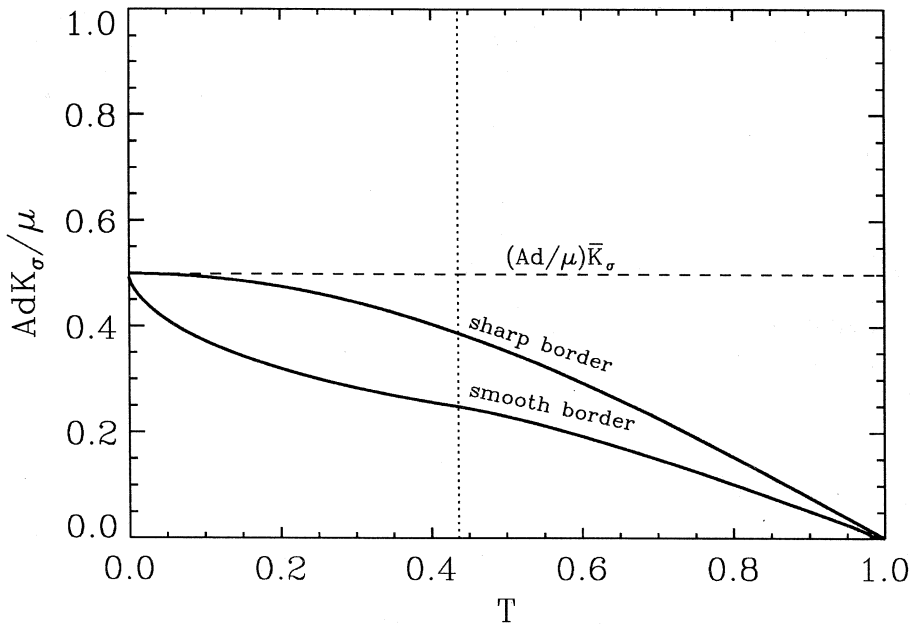

Fig. 5. Effective fault stiffness K_σ at $x = 0$ as a function of T for sharp and smooth asperity borders.

Ruina, 1985; Tullis and Weeks, 1986); however the basic effects can be discussed using a single state variable and characteristic slip distance.

We assume that the present model can reproduce the early stage of fault slip originating from a weakly coupled zone. Slip is externally driven: the dislocation area and slip enlarge due to increasing ambient shear stress. Now let us assume that slip is governed by eqs. (3.1) and (3.2). A graph of slip rate at the centre of the fault $V(T) = v(0, T)$ is shown in fig. 6, where it can be seen that the slip rate is fairly constant or slowly increasing for values of T as large as about 0.8, resulting in *steady-state slip*. During steady-state slip, it is assumed that the state variable ψ is constant in time (*e.g.* Ruina, 1983). Hence from (3.2)

$$\psi = -\ln g(v) \tag{3.3}$$

Using (3.3) in (3.1), we obtain the simplified law:

$$\kappa = \kappa_0 + (\mathcal{A} - \mathcal{B}) \ln g(v) \tag{3.4}$$

where we choose

$$g(v) = k(v - v_0) + 1 \tag{3.5}$$

where $v = v(x, T)$ and $v_0 = v(x, 0)$. The form of $g(v)$ has been chosen in order that the rate-dependent term vanishes on the fault at $T = 0$. Therefore it takes into account the case $v_0 \neq 0$, occurring in the weak zone $|x| < d$, and the case $v_0 = 0$, occurring in the asperities $|x| > d$. We choose as a reference velocity the initial slip rate V_0 at $x = 0$ and define

$$k = \frac{1}{V_0} \tag{3.6}$$

If $\mathcal{A} - \mathcal{B} < 0$, the behaviour is velocity weakening and slip may become unstable (Rice and Ruina, 1983; Gu *et al.*, 1984). In this case, friction is a decreasing function of slip rate. Multiplying (3.4) by $(\sigma_n - p)$, we obtain

$$\tau(x, T) = \tau_s(x)[1 - \gamma \ln g(v)] \tag{3.7}$$

where

$$\gamma = \frac{\mathcal{B} - \mathcal{A}}{\kappa_0} . \tag{3.8}$$

In fig. 7, friction τ on the fault is shown for some values of T in the case of asperities with sharp borders and for two values of γ. The values of γ measured in the laboratory are commonly in the range 0.01-0.001 (Dieterich, 1980, 1981; Okubo and Dieterich, 1986). Note that the shape of friction distribution is relatively unchanged with time with such small values for γ. The same result holds for asperities with smooth borders.

This enables us to approximate the constitutive eq. (3.7) for $\gamma \ll 1$. Actually the amplitude of the friction step $\tau_1 - \tau_0$ decreases with time: however this effect is small if $\gamma \ll 1$ and is neglected. At $x = 0$, (3.7) reduces to

$$\tau(0, T) = \tau_0 \left[1 - \gamma \ln \frac{V(T)}{V_0} \right] \tag{3.9}$$

where V and V_0 are slip rates at $x = 0$. Following the previous considerations, we adopt (3.9) for the whole fault surface and write

$$\tau(x, T) = \tau_s (x) F(T) \tag{3.10}$$

where

$$F(T) = 1 - \gamma \ln \frac{V(T)}{V_0} \tag{3.11}$$

This means that, at each point on the fault, friction is a decreasing function of T (or time), but the initial spatial profile remains unchanged. This approximation allows us to employ the same solution as in the absence of velocity weakening, with a remarkable simplification of calculations. Velocity weakening is

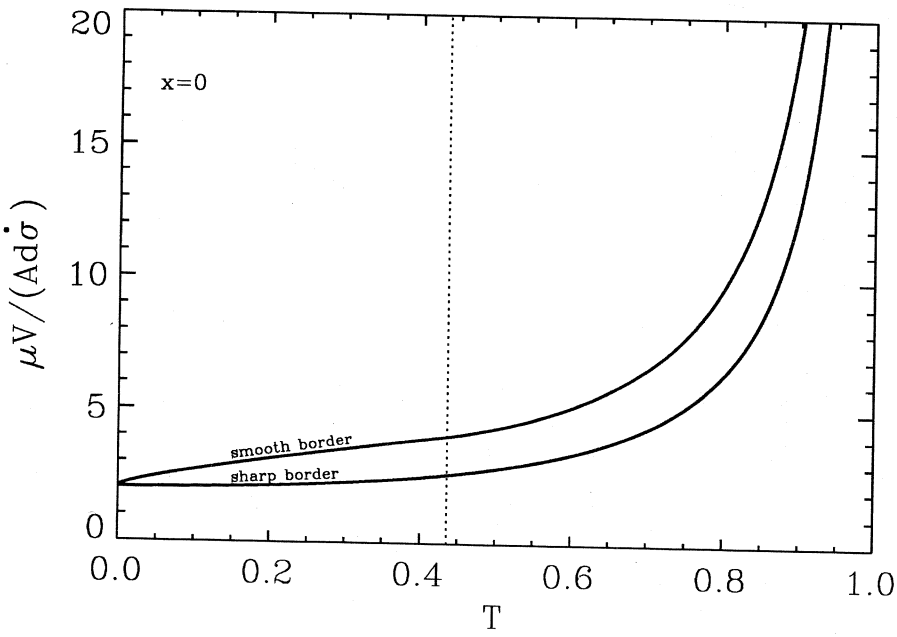

Fig. 6. Fault slip rate $V \equiv v(0, t)$ as a function of the stress parameter T for sharp and smooth asperity borders.

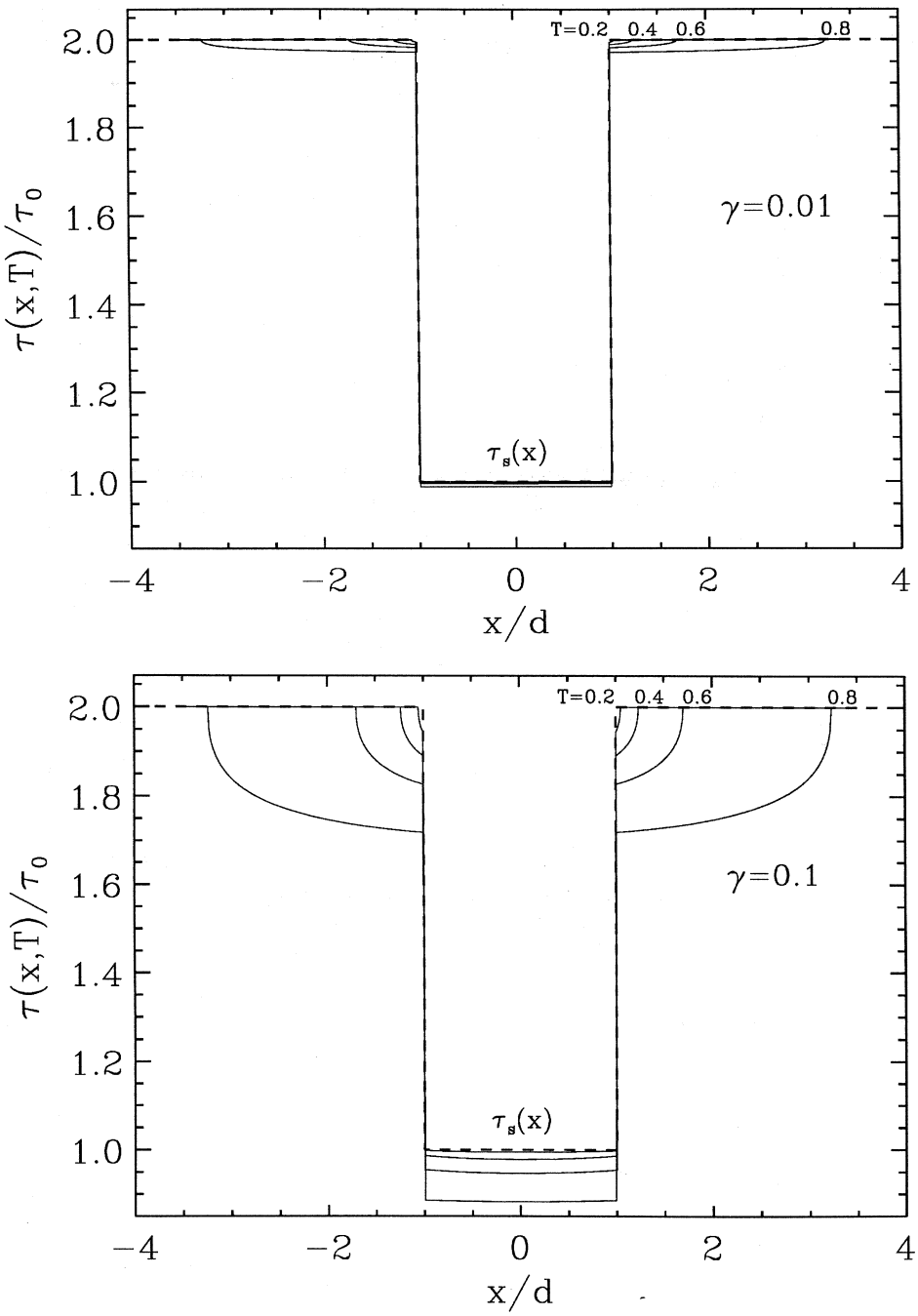

Fig. 7. Friction τ as a function of x for some values of T in the case sharp asperity borders and for two values of γ.

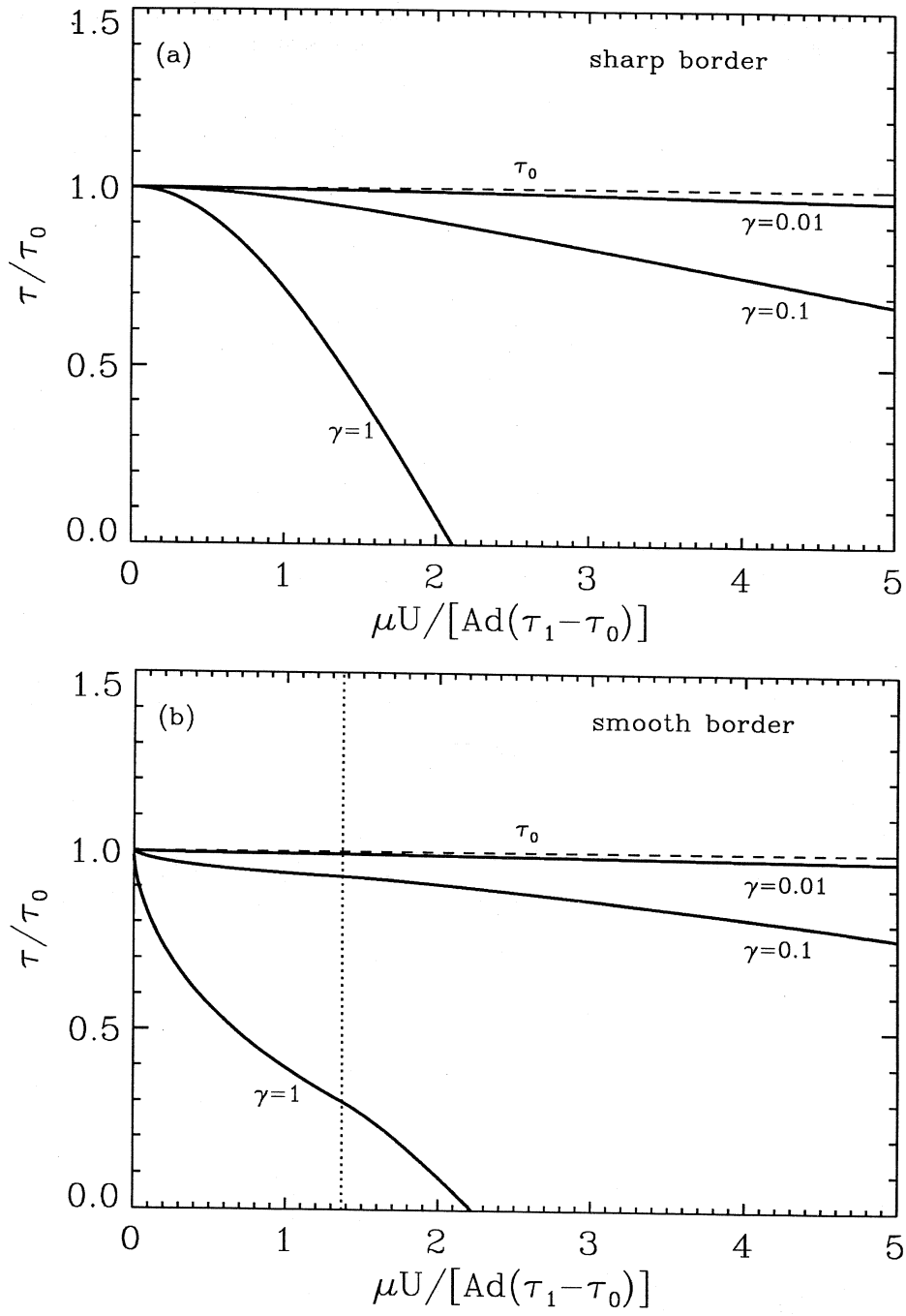

Fig. 8a,b. Friction τ as a function of fault slip U for some values of γ in the two cases of sharp asperity borders (a) and smooth asperity borders with $D = 2d$ (b).

generally expressed by:

$$\frac{d\tau}{dV} < 0 \tag{3.12}$$

From (3.10) and (3.11)

$$\frac{d\tau}{dV} = -\frac{\gamma \tau_s(x)}{V}. \tag{3.13}$$

Note that $|d\tau/dV|$ is a decreasing function of V and has a maximum at $V = V_0$.

We search for the instability conditions as a result of the competition between the decrease of friction and the possibility of the ambient stress to produce slip; therefore we consider the slip weakening induced by velocity weakening. Slip weakening is expressed by $K_\tau < 0$, where

$$K_\tau \equiv \frac{d\tau}{dU} \tag{3.14}$$

A graph of τ as a function of $\mu U/[Ad(\tau_1 - \tau_0)]$ is shown in fig. 8a,b, for some values of γ. In the case of sharp asperity borders, the slope $|K_\tau|$ is an increasing function of U, being 0 at $U = 0$. As a consequence, a given value of K_τ

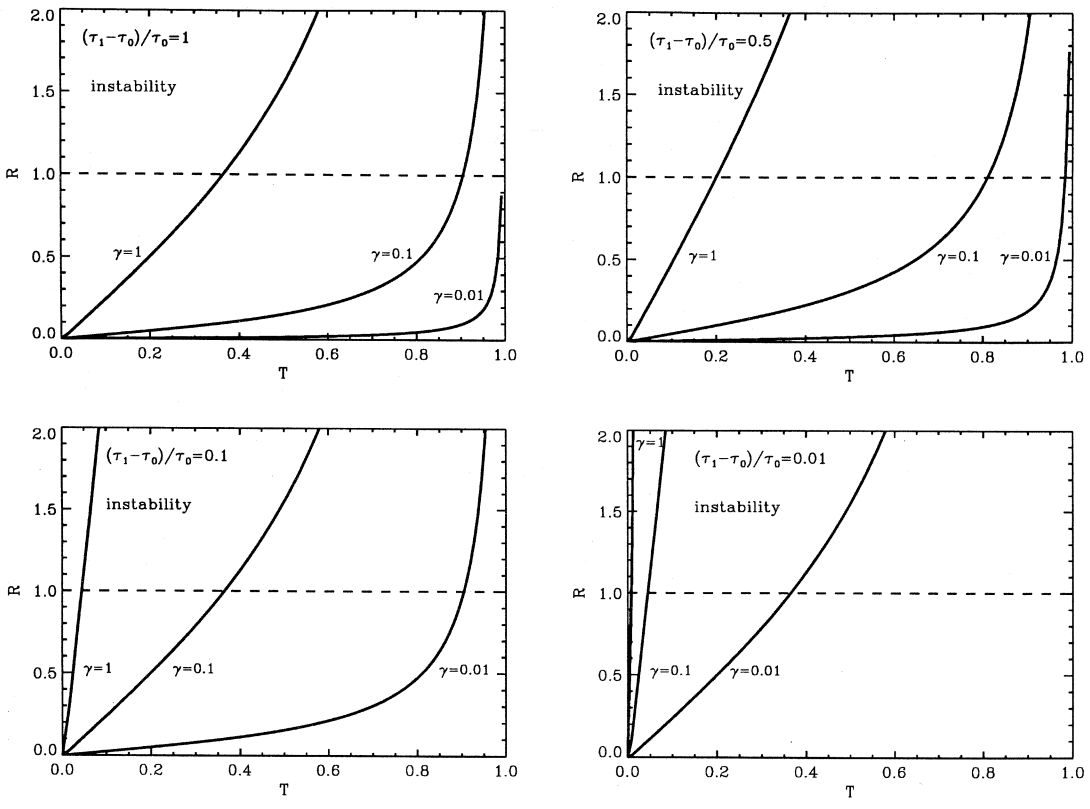

Fig. 9. Ratio R as as function of T for different values of $(\tau_1 - \tau_0) / \tau_0$ and γ for sharp asperity borders. Instability is reached when the curves for R overpass the dashed line corresponding to $R = 1$.

is reached after the fault has undergone a certain amount of slip: this is consistent with the observation of a characteristic slip distance. In the case of smooth borders we have instead that $|K_\tau|$ is decreasing until some amount of slip is achieved (dotted line) and increases only beyond this point. As a function of U, K_τ depends on γ and on the step $\tau_1 - \tau q_0$. Curves for $\gamma = 1$ are introduced as a reference, but are beyond the validity of approximation (3.10). Slip weakening is a necessary condition for instability. During slip weakening, sliding is stable as long as the rate $|K_\tau|$ at which τ decreases is less than the rate K_σ at which σ must increase to produce an advance of fault slip. On the contrary, instability occurs if the friction decrease is overwhelming: hence the condition for instability is (*e.g.* Stuart, 1981)

$$|K_\tau| > K_\sigma \tag{3.15}$$

or

$$R \equiv \frac{|K_\tau|}{K_\sigma} > 1 \tag{3.16}$$

We calculated the ratio R in the cases of static friction τ_s defined in (2.2) and (2.3), assuming a stress rate $\dot{\sigma} = \text{const}$. In fig. 9, R is plotted for sharp borders as a function of T for different values of $(\tau_1 - \tau_0)/\tau_0$ and γ. As a general rule, instability is favoured by small values of

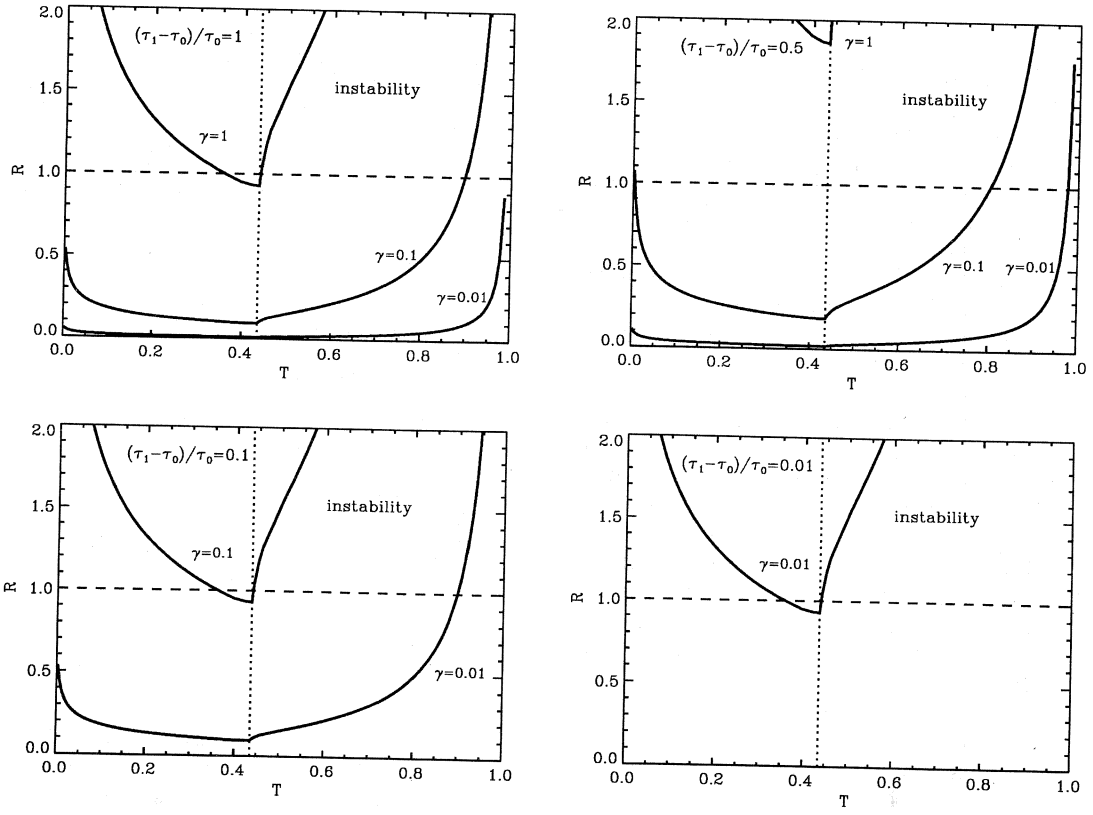

Fig. 10. Ratio R as as function of T for different values of $(\tau_1 - \tau_0)\ /\ \tau_0$ and γ for smooth asperity borders. Instability is reached when the curves for R overpass the dashed line corresponding to $R = 1$.

$\tau_1 - \tau_0$ and large values of γ. If γ is large, the friction decrease is fast and $|K_\tau|$ increases rapidly: the instability condition is reached at small values of T. If the initial slipping patch is very weak with respect to adjacent patches, the instability takes place only when friction has a relatively strong velocity dependence. Lower values of γ may lead to instability when $\tau_1 - \tau_0$ is relatively small. The values measured in the laboratory for γ are usually less than 10^{-2}, so that the corresponding curves are the most realistic if laboratory results are extrapolated to real faults. For asperities with smooth borders (fig. 10) we note the same behaviour, but as a consequence of the initial increase in $|K_\tau|$ shown in fig. 8b an instability can occur for small values of T, particularly if $\tau_1 - \tau_0$ is small.

4. Conclusions

We have studied the instability conditions on a fault by introducing an empirical constitutive law for friction into a model for stable frictional sliding under equilibrium conditions. Under a uniform ambient shear stress, slowly increasing with time, sliding starts in the weakest fault patch, being resisted by adjacent asperities. In its early stage, slip is stable and aseismic at a fairly constant rate. As the slip rate increases, friction decreases, resulting in velocity weakening. In general, the instability occurs when the rate at which friction decreases becomes greater than the rate at which the applied stress must increase to produce an advance of fault slip. The possibility that this condition is fulfilled depends on the velocity dependence and on the spatial distribution of friction on the fault: instability is favoured by a strong velocity dependence and by low strength asperities. The results indicate the crucial role played by friction inhomogeneity on a fault. Fairly different results are found in the two cases considered in this paper, sharp and smooth asperity borders. While in the first case some amount of slip is necessary before the instability takes place, this condition may not be essential in the second case.

REFERENCES

Angevine, C.L., D.L. Turcotte and M.D. Furnish (1982): Pressure solution lithification as a mechanism for the stick-slip behavior of faults, *Tectonics*, **1**, 151-160.

Bilby, B.A. and J.D. Eshelby (1968): Dislocations and the theory of fracture, in *Fracture, an Advanced Treatise*, edited by H. Liebowitz (Academic Press, New York), vol. 1, 99-182.

Bonafede, M., M. Dragoni and E. Boschi (1985): Quasi-static crack models and the frictional stress threshold criterion for slip arrest, *Geophys. J. R. Astron. Soc.*, **83**, 615-637.

Brace, W.F. and J.D. Byerlee (1966): Stick-slip as a mechanism for earthquakes, *Science*, **153**, 990-992.

Dieterich, J.H. (1978): Time-dependent friction and the mechanism of stick-slip, *Pure Appl. Geophys.*, **116**, 790-806.

Dieterich, J.H. (1979a): Modeling of rock friction, 1. Experimental results and constitutive equations, *J. Geophys. Res.*, **84**, 2161-2168.

Dieterich, J.H. (1979b): Modeling of rock friction, 2. Simulation of preseismic slip, *J. Geophys. Res.*, **84**, 2169-2175.

Dieterich, J.H. (1980): Experimental and model study of fault constitutive properties, in *Solid Earth Geophysics and Geothecnology*, Appl. Mech. Div., edited by S. Nemat-Nasser, American Society of Mechanical Engineers, New York, N.Y., 42, 21-30.

Dieterich, J.H. (1981): Constitutive properties of faults with simulated gouge, in *Mechanical Behavior of Crustal Rocks*, edited by N.L. Carter, M. Friedman, J.M. Logan and D.W. Stearns, Am. Geophys. Union, Geophys. Monogr., 24, 103-120.

Dieterich, J.H. (1986): A model for the nucleation of earthquake slip, in *Earthquake Source Mechanics*, edited by S. Das, J. Boatwright and C.H. Scholz, Amer. Geophys. Union, Washington, 37-47.

Dieterich, J.H. (1992): Earthquake nucleation on faults with rate- and state-dependent strenght, *Tectonophysics*, **211**, 115-134.

Dragoni, M. (1990): A model of interseismic fault slip in the presence of asperities, *Geophys. J. Int.*, **101**, 147-156.

Dragoni, M. (1992): A dislocation model of aseismic fault slip under nonuniform friction, *Terra Nova*, **4**, 501-508.

Dragoni, M. (1993): Stable fault sliding and earthquake nucleation, in *Recent Evolution and Seismicity of the Mediterranean Region* edited by E. Boschi, E. Mantovani and A. Morelli (Kluwer Academic Publishers, Dordrecht), 347-365.

Dragoni, M. and A. Piombo (1993): Propagation of an aseismic dislocation through asperities with smooth borders, *Phys. Earth Planet. Int.*, **80**, 1-11.

Erdogan, F., G.D. Gupta and T.S. Cook (1973): Numerical solution of singular integral equations, in *Mechanics of Fracture*, edited by G.C. Sih (Noordhoff, Leyden), vol. 1, chapt. 7.

Gu, J.C., J.R. Rice, A.L. Ruina and S.T. Tse (1984): Slip motion and stability of a single degree of freedom elastic system with rate and state dependent friction, *J. Mech. Phys. Sol.*, **32**, 167-196.

HOROWITZ, F. and A. RUINA (1985): Frictional slip patterns generated in a spatially homogeneous elastic fault model, *EOS*, **66**, 1069.

MATSU'URA, M., H. KATAOKA and B. SHIBAZAKI (1992): Slip-dependent friction law and nucleation processes in earthquake rupture, *Tectonophysics*, **211**, 135-148.

OKUBO, P.G. (1989): Dynamic rupture modeling with laboratory-derived constitutive relations, *J. Geophys. Res.*, **94**, 12321-12335.

OKUBO, P.G. and J.H. DIETERICH (1986): State variable fault constitutive relations for dynamic slip, in *Earthquake Source Mechanics*, edited by S. DAS, J. BOATWRIGHT and C.H. SCHOLZ, Amer. Geophys. Union, Washington, 25-35.

PATERSON, M.S. (1978): *Experimental Rock Deformation – The Brittle Field* (Springer-Verlag, Berlin).

RICE, J.R. (1983): Constitutive relations for fault slip and earthquake instabilities, *Pure Appl. Geophys.*, **121**, 443-475.

RICE, J.R. and D.A. SIMONS (1976): The stabilization of spreading shear faults by coupled deformation-diffusion effects in fluid-infiltrated porous materials, *J. Geophys. Res.*, **81**, 5322-5334.

RICE, J.R. and A.L. RUINA (1983): Stability of steady frictional slipping, *J. Appl. Mech.*, **105**, 343-349.

RUINA, A. (1983): Slip instability and state variable friction laws, *J. Geophys. Res.*, **88**, 10359-10370.

SCHOLZ, C.H. (1990): *The Mechanics of Earthquakes and Faulting* (Cambridge University Press, Cambridge).

SHIBAZAKI, B. and M. MATSU'URA (1992): Spontaneous processes for nucleation, dynamical propagation, and stop of earthquake rupture, *Geophys. Res. Lett.*, **19**, 1189-1192.

STUART, W.D. (1981): Stiffness method for anticipating earthquakes. *Bull. Seismol. Soc. Am.*, **71**, 363-370.

TULLIS, T.E. and J.D. WEEKS (1986): Constitutive behavior and stability of frictional sliding of granite, *Pure Appl. Geophys.*, **124**, 383-414.

WANG, C.-Y. (1984): On the constitution of the San Andreas fault zone in Central California, *J. Geophys. Res.*, **89**, 5858-5866.

WEEKS, J.D. and T.E. TULLIS (1985): Frictional sliding in dolomite: a variation in constitutive behavior, *J. Geophys Res.*, **90**, 7821-7826.

Appendix

Let us consider a fault plane embedded in an infinite elastic medium with shear modulus μ and Poisson modulus ν. Consider the x direction along the fault plane and let $\Delta\sigma(x, t)$ be the shear stress gradually released by a dislocation process according to the equilibrium equation (*e.g.* Bilby and Eshelby, 1968)

$$\Delta\sigma(x, t) - \frac{\mu b}{2\pi A} \int_{-a(t)}^{a(t)} \frac{\mathcal{D}(\xi, t)}{x - \xi} d\xi = 0, \quad |x| < a(t) \tag{A.1}$$

where $\mathcal{D}$ is a distribution of infinitesimal dislocations, each having Burgers' vector $b\mathcal{D}\,d\xi$, and $A = 1$ or $1 - \nu$ for antiplane or inplane deformation, respectively.

The Somigliana dislocation problem can be solved analytically by employing a solution technique based on Chebyshev polynomials (Erdogan *et al.*, 1973; Bonafede *et al.*, 1985). A detailed solution is given in Dragoni (1990). Here only a few points are recalled. After making the change of variable

$$y = x / a \tag{A.2}$$

where a is the dislocation half-width, the stress release $\Delta\sigma(ay, t)$ on the dislocation surface ($|y| \leq 1$) can be expanded into Chebyshev polynomials of the second kind $U_n(y)$:

$$\Delta\sigma(ay, t) = \frac{\mu}{2A} \sum_{n=1}^{\infty} \alpha_n(t)\, U_{n-1}(y) \tag{A.3}$$

where

$$U_{n-1}(y) = \frac{\sin n\theta}{\sin \theta} \tag{A.4}$$

with $\theta = \arccos y$. The evaluation of the Chebyshev coefficients with $\Delta\sigma$ given by (2.5) yields in the case of asperities with sharp borders:

$$\alpha_n(t) = \frac{2A}{\pi\mu}(\tau_1 - \tau_0)\begin{cases}\sin 2\varphi, & n = 1\\ 2\sin\dfrac{n\pi}{2}\left[\dfrac{\sin(n-1)\varphi}{n-1} + \dfrac{\sin(n+1)\varphi}{n+1}\right], & n > 1\end{cases} \tag{A.5}$$

where τ_1 and τ_0 are defined in (2.2) and

$$\varphi(t) = [1 - T(t)]\frac{\pi}{2}, \quad 0 \le T < 1 \tag{A.6}$$

while in the case of smooth borders (Dragoni and Piombo, 1993):
for $d \le a(t) \le D$,

$$\alpha_n(t) = -\frac{A}{\pi\mu} fd\left\{\frac{a}{d}\left[J_n(\theta_2^-) + J_n(\theta_2^+) - \pi\delta_{n2}\right] + 2\left[I_n(\theta_2^-) - I_n(\theta_2^+) - \pi\delta_{n1}\frac{\sigma - \tau_0 + fd}{fd}\right]\right\}, \tag{A.7}$$

for $a(t) \ge D$,

$$\begin{aligned}\alpha_n(t) = {} & \frac{2A}{\pi\mu} fd\left\{[I_n(\theta_1^-) - I_n(\theta_1^+)] - [I_n(\theta_2^-) - I_n(\theta_2^+)]\right\}\\ & + \frac{A}{\pi\mu} fa\left\{[J_n(\theta_1^-) + J_n(\theta_1^+)] - [J_n(\theta_2^-) + J_n(\theta_2^+)]\right\}\\ & + \frac{2A}{\pi\mu}(\tau_1 - \tau_0)\left\{[I_n(\theta_1^-) - I_n(\theta_1^+)] - \pi\delta_{n1}\frac{\tau_1 - \sigma}{\tau_1 - \tau_0}\right\}\end{aligned} \tag{A.8}$$

where

$$I_k(\theta) = \begin{cases}k = 1, & \theta - \dfrac{1}{2}\sin 2\theta\\ k > 1, & \dfrac{\sin(k-1)\theta}{k-1} - \dfrac{\sin(k+1)\theta}{k+1}\end{cases} \tag{A.9}$$

$$J_k(\theta) = \begin{cases}k = 2, & \theta - \dfrac{1}{4}\sin 4\theta\\ k \ne 2, & \dfrac{\sin(k-2)\theta}{k-2} - \dfrac{\sin(k+2)\theta}{k+2}\end{cases} \tag{A.10}$$

$$\theta_1^{\pm} = \arccos\left(\pm\frac{D}{a}\right), \tag{A.11}$$

$$\theta_2^{\pm} = \arccos\left(\pm \frac{d}{a}\right) \tag{A.12}$$

where τ_1 and τ_0 are defined in (2.3) and f is defined in (2.4). The slip amplitude u is then computed according to

$$u(ay, t) = a(t)\sqrt{1-y^2} \sum_{n=1}^{\infty} \frac{\alpha_n(t)}{n} U_{n-1}(y) \tag{A.13}$$

where $|y| \leq 1$. In the case of sharp borders $a(t)$ is given by

$$a(t) = d \csc \varphi(t) \tag{A.14}$$

where φ is defined in (A.6). In the case of smooth borders $a(t)$ is obtained by inverting the expressions for T:

$$T = F\left[\frac{2}{\pi}(\phi_2 - \cot \phi_2) - 1\right], \quad \text{for} \quad d \leq a(t) \leq D, \tag{A.15}$$

$$T = 1 - \frac{2}{\pi}\left[\phi_1 + F(\phi_1 - \phi_2) + F\frac{\cos\phi_1 - \cos\phi_2}{\sin\phi_2}\right], \quad \text{for} \quad a(t) \geq D, \tag{A.16}$$

where

$$F = \frac{d}{D-d}, \tag{A.17}$$

$$\phi_1 = \arcsin\frac{D}{a}, \tag{A.18}$$

$$\phi_2 = \arcsin\frac{d}{a}. \tag{A.19}$$

The slip rate $v = \dot{u}$ can be computed by differentiation of the series in (A.13) term by term. Its value at $x = 0$ is

$$v(0, t) = \sum_{n=1}^{\infty} \frac{\dot{a}(t)\alpha_n(t) + a(t)\dot{a}_n(t)}{n} U_{n-1}(0) \tag{A.20}$$

where, in the case of sharp borders,

$$\dot{\alpha}_n(t) = \frac{2A}{\mu}\dot{\sigma}\begin{cases} \cos 2\varphi, & n = 1 \\ 2\cos n\varphi \cos\varphi \sin n\frac{\pi}{2}, & n > 1 \end{cases} \tag{A.21}$$

$$\dot{a}(t) = \frac{\pi}{2}\frac{\cos\varphi}{\tau_1 - \tau_0}\frac{a^2}{d}\dot{\sigma}; \tag{A.22}$$

in the case of smooth borders, for $d \leq a(t) \leq D$

$$\dot{\alpha}_n(t) = -\frac{A}{\pi\mu} fd \left\{ \frac{\dot{a}(t)}{d} \left[J_n(\theta_2^-) + J_n(\theta_2^+) - \pi\delta_{n2} \right] - \frac{2\pi}{fd} \delta_{n1} \dot{\sigma} \right\}, \tag{A.23}$$

$$\dot{a}(t) = \frac{\pi}{2} \frac{\dot{\sigma}}{\tau_1 - \tau_0} \frac{d}{\cos\phi_2}, \tag{A.24}$$

for $a(t) \geq D$

$$\dot{\alpha}_n(t) = \frac{16A}{\pi\mu} \left(f - \frac{\tau_1 - \tau_0}{d} \right) \frac{d^2}{a^2(t)} \dot{a}(t) \sin n\frac{\pi}{2} \cos n\phi_1 + \frac{2A}{\mu} \delta_{n1} \dot{\sigma}$$

$$+ \frac{A}{\pi\mu} f\dot{a}(t) \left\{ \left[J_n(\theta_1^-) + J_n(\theta_1^+) \right] - \left[J_n(\theta_2^-) + J_n(\theta_2^+) \right] \right\}, \tag{A.25}$$

$$\dot{a}(t) = \frac{\pi}{2} \frac{\dot{\sigma}}{\tau_1 - \tau_0} \frac{d}{\cos\phi_2 - \cos\phi_1}. \tag{A.26}$$

The dot on symbols indicates differentiation with respect to time. No stress singularities are present in the solution.